PHYSICAL REVIEW B VOLUME 16, NUMBER 5 1 SEPTEMBER 1977

Magnetization studies in transition-metal niobates. II. $FeNb_2O_6$

I. Yaeger* and A. H. Morrish
Department of Physics, University of Manitoba, Winnipeg, Canada

B. M. Wanklyn and B. J. Garrard
Clarendon Laboratory, Oxford, England

(Received 21 March 1977)

The magnetization and susceptibility of flux-grown $FeNb_2O_6$ single crystals have been measured from 80 K down to 1.4 K. An antiferromagnetic ordering was observed at $T_N = 5.5 \pm 0.5$ K. The antiferromagnetic-paramagnetic phase transition induced by an external field along the orthorhombic $\vec{a}$ axis seems to be of second order in the whole range from the T_N down to 1.4 K. The experimental results are interpreted in the mean-field approximation using a four-sublattice model for the Fe^{2+} spins. A nearly accidental doublet ground state is assumed for the Fe^{2+} ions. The g tensors are found to be $g = 7.7 \pm 0.4$ in the $\vec{a}$-$\vec{c}$ plane at angles of $\pm (17^0 \pm 3^0)$ to the $\vec{a}$ axis. These are also the two easy directions of the four-sublattice Fe^{2+} spin system. The Fe^{2+}-Fe^{2+} interaction is essentially of the exchange type with a small dipolar contribution. The intrasublattice ferromagnetic interaction is found to be larger than the intersublattice antiferromagnetic coupling.

I. INTRODUCTION

$FeNb_2O_6$ and other transition-metal niobates crystallize in an orthorhombic columbite form (space group $D_{2h}^{14} - Pbcn$) with four formula units per crystallographic unit cell.[1] In the notation adopted throughout here the lattice constants of $FeNb_2O_6$ are $a = 14.2630$ Å, $b = 5.7318$ Å, and $c = 5.0378$ Å.[2] The Fe^{2+} ions are arranged in Fe-O layers containing the orthorhombic $\vec{b}$ and $\vec{c}$ axes and are separated from neighboring layers along the $\vec{a}$ axis by two nonmagnetic Nb-O layers.[2] The exchange interactions are consequently expected to be dominantly between the Fe^{2+} ions within the layers as compared with interlayer interactions.

From neutron-diffraction studies of powder samples at 4.2 K it has been concluded that $FeNb_2O_6$ orders antiferromagnetically with a collinear spin arrangement along the crystallographic $\vec{a}$ axis.[3] The magnetic ordering was found to be associated with a doubling of the unit cell along the $\vec{b}$ direction.[3]

In this paper, we report for the first time, magnetic studies of $FeNb_2O_6$ in a single-crystal form. The experimental susceptibility and induced magnetization along the orthorhombic crystallographic axes are presented in Sec. II. In Sec. III, we apply group-theory considerations to determine the g-tensor components and the representations of the possible magnetic structures of the Fe^{2+} ions. The temperature dependence of the magnetic susceptibility along the principal crystallographic directions is analyzed in Sec. IV. In the discussion that follows in the last section, some implications of the model adopted in the analysis are pointed out and reference is made to various results on powder material reported in the literature.

II. EXPERIMENTAL

The field-induced magnetization and susceptibility along the principal crystallographic directions of flux-grown single crystals of $FeNb_2O_6$ (weighing a few tens of milligrams)[4] have been measured from 80 down to 1.4 K. A PAR vibrating-sample magnetometer model FM-1 was used to measure the magnetic moment in the direction of the external field. At temperatures above 4.2 K the sample was cooled by a stream of helium gas inside a metal cryostat, and constant temperatures were maintained by using a heating coil to balance the cooling effect of the helium stream. The temperature was recorded by an Au(0.03-at.% Fe) versus chromel-P thermocouple. At 4.2 K and lower temperatures the sample was immersed in pumped liquid helium in a glass cryostat and the temperature was controlled by monitoring the vapor pressure over the liquid helium. The temperature in that range was measured using a calibrated Ge resistor. The experimental results reported here were compiled from (i) magnetization measurements versus temperature recorded at various fixed magnetic fields while heating or cooling the sample and (ii) curves of magnetization versus applied field recorded at fixed temperatures.

The susceptibility curves of $FeNb_2O_6$ along the principal crystallographic directions are shown in Fig. 1. The antiferromagnetic ordering, associated with the maximum in $d\chi/dT$, takes place at $T_N = 5.5 \pm 0.5$ K. In the $\vec{a}$-$\vec{c}$ plane the principal susceptibilities exhibit a very similar temperature dependence, whereas in the $\vec{b}$ direction there is little temperature dependence, especially at low temperatures. This suggests that the $\vec{b}$ axis

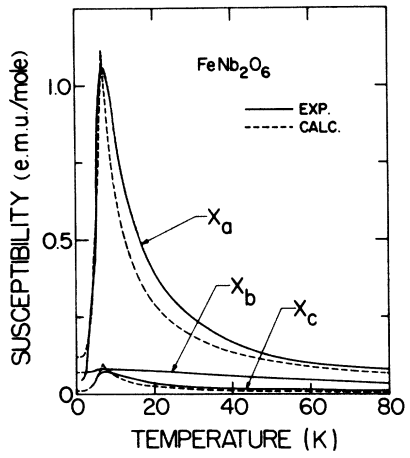

FIG. 1. Principal magnetic susceptibilities of $FeNb_2O_6$ as a function of temperature. The subscripts a,b,c refer to the orthorhombic crystallographic axes.

susceptibility is dominantly of the Van Vleck type and that the g tensor of the lowest-lying crystal-field levels of the Fe^{2+} ions in the $\vec{b}$ direction is probably zero. Also, the striking similarity in the temperature dependence of the susceptibilities along the $\vec{a}$ and $\vec{c}$ directions indicates that at each one of the two magnetically nonequivalent sites of the Fe^{2+} ions the g tensor is nonzero along only one of its principal directions in the $\vec{a}$-$\vec{c}$ plane.[5] Judging from the magnitudes of the $\vec{a}$ and $\vec{c}$ susceptibilities, this nonzero direction in the $\vec{a}$-$\vec{c}$ plane is close to the crystallographic $\vec{a}$ axis at each site. A g tensor with only one nonzero component has been found by Griffith to be characteristic

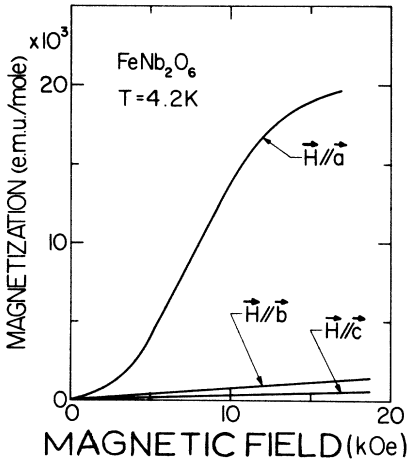

FIG. 2. Magnetization of $FeNb_2O_6$ as a function of an applied magnetic field along the orthorhombic $\vec{a}$, $\vec{b}$, and $\vec{c}$ directions at 4.2 K.

of a nearly accidental doublet.[6] A magnetic susceptibility similar in its temperature dependence to that of $FeNb_2O_6$ was found also in $HoCrO_3$ where the dominant contribution to the low-temperature susceptibility comes from the Ho^{3+} ions that have a nearly accidental ground doublet.[7] In the analysis of the experimental data we shall, therefore, assume that the Fe^{2+} ions in $FeNb_2O_6$ have a nearly accidental ground doublet.

In the magnetization versus field curves (Fig. 2) an antiferromagnetic-paramagnetic (AF-PM) field-induced phase transition was found to take place in the temperature range below T_N when the external field was applied along the crystallographic $\vec{a}$ axis. The transition seemed to be of second order down to 1.4 K. No indication of field-induced transitions was found with the external field along the two other crystallographic directions for fields up to 19 kOe. This can be regarded as further evidence that the easy directions of the Fe^{2+} spins at the two magnetically nonequivalent sites are close to, or coincide with the crystallographic $\vec{a}$ axis. Field-induced transitions in $FeNb_2O_6$ at $T = 0.34$ K that will be reported and analyzed elsewhere[8] tend to indicate a noncollinear Fe^{2+} spin structure.

III. GROUP-THEORY TREATMENT

In this section we shall relate the g tensors of the Fe^{2+} ions at the two magnetically nonequivalent sites[5] to the transformation properties of their nearly accidental ground-doublet states under the site-symmetry operations. Further, representations belonging to the space group $Pbcn$ will be derived for all the possible magnetic structures of the Fe^{2+} spins originating from the doubling of the unit cell along the $\vec{b}$ direction found in neutron-diffraction studies of powder material.[3]

A. g tensor of the Fe^{2+} ions in the nearly accidental ground doublet

The Fe^{2+} ions occupy the $4(c)$ sites in the crystallographic unit cell. Their locations are (1) $0\,y\,\frac{1}{4}$, (2) $0\,\bar{y}\,\frac{3}{4}$, (3) $\frac{1}{2}\,\frac{1}{2}-y\,\frac{3}{4}$, and (4) $\frac{1}{2}\,\frac{1}{2}+y\,\frac{1}{4}$ with $y = 0.1456$ (see Fig. 3).[3] As it was shown in the crystallographically isotructural $NiNb_2O_6$,[5] the $4(c)$ sites comprise two types of magnetically nonequivalent sites. Sites 1 and 2 are magnetically of one type whereas sites 3 and 4 are of the other type. The general form and principal axes of the g tensors of the Fe^{2+} ions at the two types of magnetically nonequivalent sites in $FeNb_2O_6$ are also similar to those found for Ni^{2+} ions[5] in $NiNb_2O_6$ (Fig. 4). However, in case of a nearly accidental doublet further restrictions apply to the g tensor. It was found by Griffith[6] that a nearly accidental

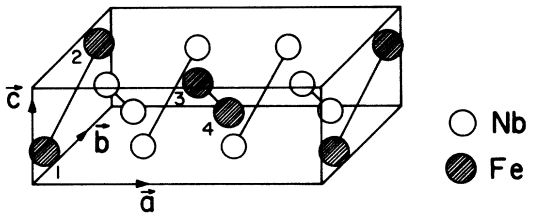

FIG. 3. Crystallographic unit cell of $FeNb_2O_6$. Fe^{2+} ions occupy the 4(c) sites at (1) $0y\frac{1}{4}$ (2) $0\bar{y}\frac{3}{4}$ (3) $\frac{11}{22}-y\frac{3}{4}$ and (4) $\frac{11}{22}+y\frac{1}{4}$.

doublet has a g factor along only one direction and the g factor in orthogonal directions is strictly zero. The direction of the only g factor is along the vector $\vec{g}$ given by

$$\vec{g}=2\langle a|\vec{L}+2\vec{S}|b\rangle \ . \tag{1}$$

$|a\rangle$ and $|b\rangle$ are the crystal-field states that comprise the doublet and $\vec{L}$ and $\vec{S}$ are the total orbital and spin angular-momentum operators, respectively.

The nonzero direction of the g factor can be determined both from the transformation properties of $|a\rangle$ and $|b\rangle$ and from the site symmetry. The site symmetry of the Fe^{2+} ions is 2_y, namely a twofold axis parallel to the crystallographic $\vec{b}$ axis. Therefore, the crystal field states must transform according to one of the two representations of 2_y. The representation of 2_y and the vector and angular-momentum components belonging to these representations are given by

$$\begin{array}{lcccc} & & 1 & 2_y & \\ y,\ J_y & A_1 & 1 & 1 & \\ x,\ z,\ J_x,\ J_z & A_2 & 1 & -1 & . \end{array} \tag{2}$$

It is evident that if the two states belong to the same representation the g vector is directed along the crystallographic $\vec{b}$ axis. On the other hand, if the two states belong to different representations, the g vector lies in the crystallographic $\vec{a}$-$\vec{c}$ plane. From the experimental data it is clear that the latter case applies to Fe^{2+} in $FeNb_2O_6$.

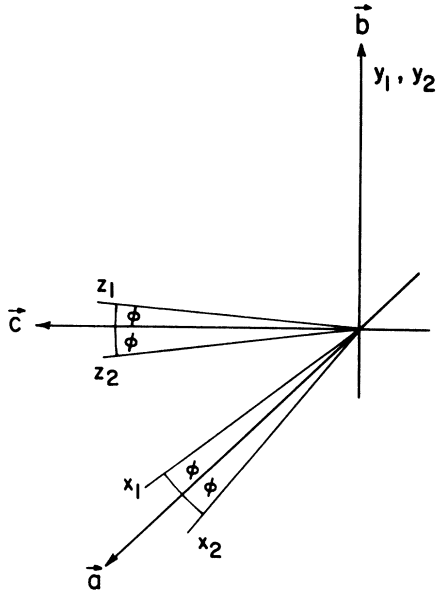

FIG. 4. Local principal axes x_i, y_i, z_i of the g tensor of magnetic ions occupying the two types of magnetically nonequivalent 4(c) sites in *Pbcn*. $\vec{a}$, $\vec{b}$, and $\vec{c}$ mark the orthorhombic crystallographic axes.

B. Irreducible representations of *Pbcn* associated with $\vec{k}=[0\frac{1}{2}0]$

1. Operators in Pbcn

Here we shall essentially follow the Olbrychski[9] method. It will be applied to *Pbcn* when the $\vec{k}$ vectors have the full point symmetry of the space group, namely, *mmm*.

As generators of the space group we select 2_{1x} at $x\frac{1}{4}0$, 2_y at $0y\frac{1}{4}$ and $\bar{1}$ at 000. These operators can be written in the form

$$2_{1x}=\{2_x|\vec{\tau}_x\},\quad 2_y=\{2_y|\vec{\tau}_y\},\quad \bar{1}=\{I|0\}; \tag{3}$$

where 2_x, 2_y are twofold axes and I is the inversion and

$$\vec{\tau}_x=\begin{pmatrix}\frac{1}{2}\\ \frac{1}{2}\\ 0\end{pmatrix} \text{ and } \vec{\tau}_y=\begin{pmatrix}0\\ 0\\ \frac{1}{2}\end{pmatrix} \ . \tag{4}$$

The point group *mmm* is defined by the following multiplication relations:

$$2_x^2=2_y^2=I^2=e,\quad 2_x2_y=2_y2_x,\quad 2_xI=I2_x, \tag{5}$$

where e is the identity operator. The corresponding relations between the generators of the space group *Pbcn* read as follows:

$$\begin{aligned} &2_{1x}^2=\{e|\vec{t}_1\} \text{ with } \vec{t}_1=(2_x+e)\vec{\tau}_x \ , \\ &2_y^2=\{e|\vec{t}_2\} \text{ with } \vec{t}_2=(2_y+e)\vec{\tau}_y, \\ &\bar{1}^2=\{e|\vec{t}_3\} \text{ with } \vec{t}_3=0, \\ &2_{1x}\bar{1}=\{e|\vec{t}_{13}\}\bar{1}2_{1x} \text{ with } \vec{t}_{13}=2\vec{\tau}_x, \\ &2_y\bar{1}=\{e|\vec{t}_{23}\}\bar{1}2y \text{ with } \vec{t}_{23}=2\vec{\tau}_y, \\ &2_{1x}2_y=\{e|\vec{t}_{12}\}2_y2_{1x} \text{ with } \vec{t}_{12}=(e-2_y)\vec{\tau}_x+(2_x-e)\vec{\tau}_y. \end{aligned} \tag{6}$$

The point transformation of sites 4(c) by the generators of *Pbcn* is given in Table I.

2. Representations in Pbcn

Let us denote by A_1, A_2, and A_3 the matrices representing 2_{1x}, 2_y, and $\bar{1}$, respectively. A

TABLE I. Point transformation of sites 4(c) in *Pbcn*. (1) $0y\frac{1}{4}$, (2) $0\bar{y}\frac{3}{4}$, (3) $\frac{1}{2}\frac{1}{2}-y\frac{3}{4}$, and (4) $\frac{1}{2}\frac{1}{2}+y\frac{1}{4}$:

2_{1x} at $x\frac{1}{4}0$; 2_y at $0y\frac{1}{4}$; $\bar{1}$ at 000.

2_{1x} transforms point 1 to 3 plus a translation $(0,0,\bar{1})$, point 2 to 4 plus a translation $(0,0,\bar{1})$, point 3 to 1 plus a translation $(1,0,\bar{1})$ and point 4 to 2 plus a translation $(1,0,\bar{1})$.

1	2_{1x}	2_y	$\bar{1}$
1	$3(00\bar{1})$	1	$2(00\bar{1})$
2	$4(00\bar{1})$	$2(00\bar{1})$	$1(00\bar{1})$
3	$1(10\bar{1})$	$3(\bar{1}0\bar{1})$	$4(\bar{1}\bar{1}\bar{1})$
4	$2(10\bar{1})$	$4(\bar{1}00)$	$3(\bar{1}\bar{1}\bar{1})$

translation $\vec{t}$ is represented by $1\times\exp(2\pi i\vec{k}\cdot\vec{t})$ (where 1 is the unit matrix) in the space-group representation associated with the wave vector $\vec{k}$. The relations between the generators of the space group imply the following relations between the representing matrices:

$$A_j^2=\epsilon_j\times 1,\quad A_iA_j=A_jA_i\,\epsilon_{ij},\quad i,j=1,2,3; \tag{7}$$

with

$$\epsilon_j=\exp(2\pi i\vec{k}\cdot\vec{t}_j);\quad \epsilon_{ij}=\exp(2\pi i\vec{k}\cdot\vec{t}_{ij})\ . \tag{8}$$

Knowing $\vec{\tau}_x$ and $\vec{\tau}_y$, the translations $\vec{t}_j$ and $\vec{t}_{ij}$ $(i,j=1,2,3)$ can be derived. This yields the following ϵ_j and ϵ_{ij} $(i,j=1,2,3)$ in the space group *Pbcn*

$$\begin{aligned}&\epsilon_1=\exp(2\pi i k_1);\quad \epsilon_2=1;\quad \epsilon_3=1\ ,\\ &\epsilon_{12}=\exp[2\pi i(k_1-k_3)],\\ &\epsilon_{13}=\exp[2\pi i(k_1+k_2)],\\ &\epsilon_{23}=\exp(2\pi i k_3)\ ,\end{aligned} \tag{9}$$

where k_j $(j=1,2,3)$ are the components of the wave vector $\vec{k}$

$$\vec{k}=k_1\vec{b}_1+k_2\vec{b}_2+k_3\vec{b}_3\ . \tag{10}$$

The phase factors ϵ_j and ϵ_{ij} for $\vec{k}$ vectors which have the full point group symmetry are given in Table II.

3. *Doubling of the Pbcn unit cell in the* $\vec{b}$ *direction*

a. Irreducible representations of Pbcn with $\vec{k}=[0\frac{1}{2}0]$. Let us take A_1 and A_2 diagonal and write the representation matrices in the following way:

$$A_1=\begin{pmatrix}x&0\\0&y\end{pmatrix},\quad A_2=\begin{pmatrix}a&0\\0&b\end{pmatrix},\quad A_3=\begin{pmatrix}z_1&z_2\\z_3&z_4\end{pmatrix}\ . \tag{11}$$

Taking into account the relations between the matrices they reduce to

$$A_1=\begin{pmatrix}x&0\\0&-x\end{pmatrix},\quad A_2=\begin{pmatrix}a&0\\0&a\end{pmatrix},\quad A_3=\begin{pmatrix}0&z_2\\z_2^{-1}&0\end{pmatrix}\ , \tag{12}$$

with $x^2=a^2=1$. If we restrict ourselves to real values of z_2 one may take for z_2, x, and a any one of the eight sign combinations ±1. This gives rise to the following eight representations:

	Γ_1'	Γ_2'	Γ_3'	Γ_4'	Γ_5'	Γ_6'	Γ_7'	Γ_8'
z_2	+1	−1	+1	+1	+1	−1	−1	−1
x	+1	+1	−1	+1	−1	+1	−1	−1
a	+1	+1	+1	−1	−1	−1	+1	−1

(13)

The representation with $z_2=x=a=+1$ has the following form:

TABLE II. Phase factors ϵ_j and ϵ_{ij} in *Pbcn*.

$\vec{k}$	ϵ_1	ϵ_2	ϵ_3	ϵ_{12}	ϵ_{23}	ϵ_{13}	Order of irreducible representations	Nature and number of irreducible representations
0	1	1	1	1	1	1	1	Real 8
$\frac{1}{2}\vec{b}_1$	−1	1	1	−1	1	−1	2	Real 2
$\frac{1}{2}\vec{b}_2$	1	1	1	1	1	−1	2	Real 2
$\frac{1}{2}\vec{b}_3$	1	1	1	−1	−1	1	2	Real 2
$\frac{1}{2}(\vec{b}_1+\vec{b}_2)$	−1	1	1	−1	1	1	2	Real 2
$\frac{1}{2}(\vec{b}_2+\vec{b}_3)$	1	1	1	−1	−1	−1	2	Real 2
$\frac{1}{2}(\vec{b}_1+\vec{b}_3)$	−1	1	1	1	−1	−1	2	Real 2
$\frac{1}{2}(\vec{b}_1+\vec{b}_2+\vec{b}_3)$	−1	1	1	1	−1	1	2	Complex 2

$$\Gamma_{1k}(=\Gamma_1'),$$

$$\begin{array}{cccccccc} e & A_1 & A_2 & A_1A_2 & A_3 & A_1A_3 & A_2A_3 & A_1A_2A_3 \\ \begin{pmatrix}1&0\\0&1\end{pmatrix} & \begin{pmatrix}1&0\\0&-1\end{pmatrix} & \begin{pmatrix}1&0\\0&1\end{pmatrix} & \begin{pmatrix}1&0\\0&-1\end{pmatrix} & \begin{pmatrix}0&1\\1&0\end{pmatrix} & \begin{pmatrix}0&1\\-1&0\end{pmatrix} & \begin{pmatrix}0&1\\1&0\end{pmatrix} & \begin{pmatrix}0&1\\-1&0\end{pmatrix} \end{array}. \tag{14}$$

Another irreducible representation (not equivalent to Γ_{1k}) is obtained by the choice $z_2 = x = -a = +1$

$$\Gamma_{2k}(=\Gamma_4'),$$

$$\begin{array}{cccccccc} e & A_1 & A_2 & A_1A_2 & A_3 & A_1A_3 & A_2A_3 & A_1A_2A_3 \\ \begin{pmatrix}1&0\\0&1\end{pmatrix} & \begin{pmatrix}1&0\\0&-1\end{pmatrix} & \begin{pmatrix}-1&0\\0&-1\end{pmatrix} & \begin{pmatrix}-1&0\\0&1\end{pmatrix} & \begin{pmatrix}0&1\\1&0\end{pmatrix} & \begin{pmatrix}0&1\\-1&0\end{pmatrix} & \begin{pmatrix}0&-1\\-1&0\end{pmatrix} & \begin{pmatrix}0&-1\\1&0\end{pmatrix} \end{array}. \tag{15}$$

All the other representations are either equivalent to Γ_{1k} or to Γ_{2k}:

$$\begin{aligned} &\Gamma_1' \sim \Gamma_2' \sim \Gamma_3' \sim \Gamma_7' \sim \Gamma_{1k}, \\ &\Gamma_4' \sim \Gamma_5' \sim \Gamma_6' \sim \Gamma_8' \sim \Gamma_{2k}. \end{aligned} \tag{16}$$

b. *Derivation of the bases of irreducible representations of Pbcn with* $\vec{k}=[0\,\frac{1}{2}\,0]$. With the unit cell doubled in the $\vec{b}$ direction we shall denote by j' a point which is displaced from the point j by one crystallographic lattice constant in the $\vec{b}$ direction. In this notation, the point transformation of sites $4(c)$ under the generators of the space group *Pbcn* is given in Table III. In Table IV the transformation of the spins on sites $4(c)$ under the generators of *Pbcn* is displayed. Given the irreducible representations Γ_{1k} and Γ_{2k} of *Pbcn* for $\vec{k}=[0\,\frac{1}{2}\,0]$, the techniques of projection operators when applied to a spin component or a suitable linear combination of spin components ψ will project out the linear combinations ψ_{ij} which form the basis of irreducible representations:

$$\psi_{ij}^{(\nu)} = \sum_g A_{ij}^{(\nu)}(C_g) \times C_g \psi. \tag{17}$$

Here, $A^{(\nu)}(C_g)$ is the matrix that represents the operator C_g in the representation Γ_ν and $A_{ij}^{(\nu)}(C_g)$ is a matrix element. The summation is over all the members g of the group.

Let us take the representation Γ_{1k} and consider for ψ the following linear-spin combinations:

$$\psi^+ = S_{1x} + S_{2x}, \quad \psi^- = S_{1x} - S_{2x}. \tag{18}$$

By using the matrices of the representation Γ_{1k} and Table IV of the spin transformations in $P_{2b}bcn$ one finds

$$\begin{aligned} &\psi_{11}^+ = 0, \quad \psi_{12}^+ = 0; \\ &\psi_{21}^+ = 0, \quad \psi_{22}^+ = 0; \\ &\psi_{11}^- = 0, \quad \psi_{12}^- = 0; \\ &\psi_{21}^- = 0, \quad \psi_{22}^- = 0. \end{aligned} \tag{19}$$

TABLE III. Point transformation in $P_{2b}bcn$ at sites $4(c)$. Primes indicate sites displaced by one lattice constant along the $\vec{b}$ direction.

1	2_{1x}	2_y	$\bar{1}$
1	$3(00\bar{1})$	1	$2(00\bar{1})$
2	$4(00\bar{1})$	$2(00\bar{1})$	$1(00\bar{1})$
3	$1(10\bar{1})$	$3(\bar{1}0\bar{1})$	$4'(\bar{1}0\bar{1})$
4	$2(10\bar{1})$	$4(\bar{1}00)$	$3'(\bar{1}0\bar{1})$
1′	$3'(00\bar{1})$	1′	$2'(00\bar{1})$
2′	$4'(00\bar{1})$	$2'(00\bar{1})$	$1'(00\bar{1})$
3′	$1'(10\bar{1})$	$3'(\bar{1}0\bar{1})$	$4'(\bar{1}0\bar{1})$
4′	$2'(10\bar{1})$	$4'(\bar{1}00)$	$3'(\bar{1}0\bar{1})$

TABLE IV. Spin transformation in $P_{2b}bcn$ at sites $4(c)$. Primes indicate sites displaced by one lattice constant along the $\vec{b}$ direction.

1	2_{1x}	2_y	$\bar{1}$
S_{1x}	S_{3x}	$-S_{1x}$	S_{2x}
S_{1y}	$-S_{3y}$	S_{1y}	S_{2y}
S_{1z}	$-S_{3z}$	$-S_{1z}$	S_{2z}
S_{2x}	S_{4x}	$-S_{2x}$	S_{1x}
S_{2y}	$-S_{4y}$	S_{2y}	S_{1y}
S_{2z}	$-S_{4z}$	$-S_{2z}$	S_{1z}
S_{3x}	S_{1x}	$-S_{3x}$	$S_{4'x}$
S_{3y}	$-S_{1y}$	S_{3y}	$S_{4'y}$
S_{3z}	$-S_{1z}$	$-S_{3z}$	$S_{4'z}$
S_{4x}	S_{2x}	$-S_{4x}$	$S_{3'x}$
S_{4y}	$-S_{2y}$	S_{4y}	$S_{3'y}$
S_{4z}	$-S_{2z}$	$-S_{4z}$	$S_{3'z}$
$S_{1'x}$	$S_{3'x}$	$-S_{1'x}$	$S_{2'x}$
$S_{1'y}$	$-S_{3'y}$	$S_{1'y}$	$S_{2'y}$
$S_{1'z}$	$-S_{3'z}$	$-S_{1'z}$	$S_{2'z}$
$S_{2'x}$	$S_{4'x}$	$-S_{2'x}$	$S_{1'x}$
$S_{2'y}$	$-S_{4'y}$	$S_{2'y}$	$S_{1'y}$
$S_{2'z}$	$-S_{4'z}$	$-S_{2'z}$	$S_{1'z}$
$S_{3'x}$	$S_{1'x}$	$-S_{3'x}$	$S_{4'x}$
$S_{3'y}$	$-S_{1'y}$	$S_{3'y}$	$S_{4'y}$
$S_{3'z}$	$-S_{1'z}$	$-S_{3'z}$	$S_{4'z}$
$S_{4'x}$	$S_{2'x}$	$-S_{4'x}$	$S_{3'x}$
$S_{4'y}$	$-S_{2'y}$	$S_{4'y}$	$S_{3'y}$
$S_{4'z}$	$-S_{2'z}$	$-S_{4'z}$	$S_{3'z}$

On turning to Γ_{2k} one has (for the notation of the spin modes see Ref. 5)

$$\begin{aligned}
&\psi_{11}^{+}=2F_x, \quad \psi_{12}^{+}=2F_x;\\
&\psi_{21}^{+}=2C_x, \quad \psi_{22}^{+}=2C_x;\\
&\psi_{11}^{-}=2G_x, \quad \psi_{12}^{-}=-2G_x;\\
&\psi_{21}^{-}=-2A_x, \quad \psi_{22}^{-}=2A_x.
\end{aligned} \tag{20}$$

The functions ψ_{ij} with a fixed j are partners in the two-dimensional representation. Considering Γ_{2k} for instance, $\psi_{12}^{+}=2F_x$ and $\psi_{22}^{+}=2C_x$ provide an equivalent description of the same physical reality with the difference being only the choice of the coordinate system.[10]

By applying projection operators also to the functions $(S_{1y}\pm S_{2y})$ and $(S_{1z}\pm S_{2z})$ one finds eventually the following results:

	Γ_{1k}	Γ_{2k}		
ϕ_1	C_y	A_y	F_x	G_x	C_z	A_z
ϕ_2	F_y	$-G_y$	C_x	$-A_x$	F_z	$-G_z$

(21)

Thus if an exact doubling of an orthorhombic magnetic configuration along the crystallographic $\vec{b}$ axis is realized in $FeNb_2O_6$ then the magnetization and susceptibility data imply that the spontaneous magnetic structure belongs to the Γ_{2k} representation.

IV. ANALYSIS

As we have already pointed out, the temperature dependence of the principal susceptibilities in $FeNb_2O_6$ exhibits some striking features characteristic of a nearly accidental doublet. In the forthcoming analysis we shall thus assume that the apparent total lifting of the degeneracy of the Fe^{2+} energy levels due to the low-site symmetry (2_y) results in a nearly accidental ground doublet. Further, it will be assumed that only the ground doublet is populated at low temperatures, namely that the population of higher levels can be neglected. The effective spin Hamiltonian to be constructed will thus be within the frame of fictitious spin $S=\frac{1}{2}$. Considering the experimental data and the properties of the g tensor of a nearly accidental doublet,[6] we shall take

$$\begin{aligned}
&g_{x1}=g_{x2}\neq 0,\\
&g_{y_i}=g_{z_i}=0, \quad i=1,2,
\end{aligned} \tag{22}$$

where $x_i\, y_i z_i$ indicate the local principal axes of the g tensor at the magnetic site i (see Fig. 4).

Due to the relatively large separation of the Fe^{2+} ions along the $\vec{a}$ axis, the exchange interactions are expected to be dominantly between Fe^{2+} ions within the $\vec{b}$-$\vec{c}$ layers. We shall neglect interlayer interactions and for that matter assume that spins 1 and 2 in the unit cell do not interact with spins 3 and 4 (Fig. 3). The effective spin Hamiltonian will then be given by $\mathcal{H}=\mathcal{H}_{12}+\mathcal{H}_{34}$, where $\mathcal{H}_{12}$ describes interactions involving spins 1 and 2 and $\mathcal{H}_{34}$ describes interactions involving spins 3 and 4. Further, since $g_{y_i}=g_{z_i}=0 (i=1,2)$ the magnetic moments of the Fe^{2+} ions that originate from the accidental doublet are only along the x_1 and x_2 directions for spins 1, 2 and 3, 4, respectively. The nearly accidental doublet can therefore contribute to the magnetic susceptibility only in the $\vec{a}$-$\vec{c}$ plane. In the following we shall neglect other contributions to the $\vec{a}$-$\vec{c}$ plane susceptibility. In the $\vec{b}$ direction, however, the susceptibility will be of the Van Vleck type.

A. Susceptibility in the $\vec{a}$-$\vec{c}$ plane

$\mathcal{H}_{12}$ and $\mathcal{H}_{34}$ can be written in the form of decoupled-spin Hamiltonians

$$\begin{aligned}
\mathcal{H}_{12}&=\sum_{j_1}\mathcal{H}_{j_1}+\sum_{j_2}\mathcal{H}_{j_2},\\
\mathcal{H}_{34}&=\sum_{j_3}\mathcal{H}_{j_3}+\sum_{j_4}\mathcal{H}_{j_4}.
\end{aligned} \tag{23}$$

Replacing indices j_i by i, $\mathcal{H}_{j_i}$ are given by the following expressions[5,6]:

$$\begin{aligned}
\mathcal{H}_1&=z_{11}\langle S_{1x_1}\rangle y_{11}S_{1x_1}+\tfrac{1}{2}z_{12}\langle S_{2x_1}\rangle y'_{11}S_{1x_1}\\
&\quad+\Delta S_{1z_1}-H_{x_1}\mu_B g_x S_{1x_1},\\
\mathcal{H}_2&=z_{22}\langle S_{2x_1}\rangle y_{11}S_{2x_1}+\tfrac{1}{2}z_{21}\langle S_{1x_1}\rangle y'_{11}S_{2x_1}\\
&\quad+\Delta S_{2z_1}-H_{x_1}\mu_B g_x S_{2x_1},\\
\mathcal{H}_3&=z_{33}\langle S_{3x_2}\rangle y_{11}S_{3x_2}+\tfrac{1}{2}z_{34}\langle S_{4x_2}\rangle y'_{11}S_{3x_2}\\
&\quad+\Delta S_{3z_2}-H_{x_2}\mu_B g_x S_{3x_2},\\
\mathcal{H}_4&=z_{44}\langle S_{4x_2}\rangle y_{11}S_{4x_2}+\tfrac{1}{2}z_{43}\langle S_{3x_2}\rangle y'_{11}S_{4x_2}\\
&\quad+\Delta S_{4z_2}-H_{x_2}\mu_B g_x S_{4x_2}.
\end{aligned} \tag{24}$$

Here, z_{kl} is the effective number of interacting l-type neighbor spins of a k-type Fe^{2+} spin, y_{11} and y'_{11} are the intrasublattice and intersublattice interaction constants, respectively, g_x is the nonzero component of the g tensor and $\langle\ \rangle$ indicates the thermal average. Note that

$$\begin{aligned}
&z_{11}=z_{22}=z_{33}=z_{44}, \quad z_{12}=z_{21}=z_{34}=z_{43},\\
&g_x=g_{x_1}=g_{x_2}.
\end{aligned} \tag{25}$$

In the following, we shall focus on $\mathcal{H}_1$ and $\mathcal{H}_2$. The treatment of $\mathcal{H}_3$ and $\mathcal{H}_4$ is similar.

$\mathcal{H}_1$ and $\mathcal{H}_2$ have the form

$$\mathcal{H}_i=\Delta S_{iz_1}-\mu_B g_x H^{\text{eff}}_{ix_1}S_{ix_1}, \tag{26}$$

where

$$H_{1x_1}^{\text{eff}} = -\frac{4}{Ng_x^2\mu_B^2}(z_{11}y_{11}M_{1x_1} + \tfrac{1}{2}z_{12}y'_{11}M_{2x_1}) + H_{x_1},$$
$$H_{2x_1}^{\text{eff}} = -\frac{4}{Ng_x^2\mu_B^2}(z_{11}y_{11}M_{2x_1} + \tfrac{1}{2}z_{12}y'_{11}M_{1x_1}) + H_{x_1}, \tag{27}$$

and

$$M_{ix_1} = \tfrac{1}{4}Ng_x\mu_B\langle S_{ix_1}\rangle, \quad i = 1, 2. \tag{28}$$

By expressing the operators S_{ix_1} and S_{ix_1} $(i = 1, 2)$ by their 2×2 matrices, the eigenvalues of $\mathcal{H}_i$ can be easily found to be

$$\lambda_1^{(i)} = [(\tfrac{1}{2}\Delta)^2 + (\tfrac{1}{2}\mu_B g_x H_{ix_1}^{\text{eff}})^2]^{1/2},$$
$$\lambda_2^{(i)} = -[(\tfrac{1}{2}\Delta)^2 + (\tfrac{1}{2}\mu_B g_x H_{ix_1}^{\text{eff}})^2]^{1/2}, \tag{29}$$

$i = 1, 2$.

The partition function z_i of spin i is thus given by

$$z_i = 2\cosh\left(\frac{1}{kT}[(\tfrac{1}{2}\Delta)^2 + (\tfrac{1}{2}\mu_B g_x H_{ix_1}^{\text{eff}})^2]^{1/2}\right). \tag{30}$$

The total partition function Z_i of all spins on sublattice i is given by

$$Z_i = z_i^{N/4}. \tag{31}$$

Also, the free energy of all the spins on sublattice i is given by

$$F_i = -kT\ln Z_i \tag{32}$$

and the sublattice magnetization can be derived from the formula

$$M_{ix_1} = -\frac{\partial F_i}{\partial H_{ix_1}^{\text{eff}}}, \quad i = 1, 2, \tag{33}$$

which yields

$$M_{ix_1} = \frac{N}{4}\frac{(\tfrac{1}{2}\mu_B g_x)^2 H_{ix_1}^{\text{eff}}}{[(\tfrac{1}{2}\Delta)^2 + (\tfrac{1}{2}\mu_B g_x H_{ix_1}^{\text{eff}})^2]^{1/2}} \times \tanh\left(\frac{1}{kT}[(\tfrac{1}{2}\Delta)^2 + (\tfrac{1}{2}\mu_B g_x H_{ix_1}^{\text{eff}})^2]^{1/2}\right). \tag{34}$$

Note that if $\Delta \neq 0$ then at finite external fields

$$M_{ix_1}(T = 0\ K) < \tfrac{1}{4}Ng_x\mu_B S. \tag{35}$$

In order to obtain an expression for the susceptibility in the x_1 direction, the formula for M_{ix_1} will be treated in the limit of H_{x_1} tending to zero. Up to the first power of H_{x_1} one has

$$M_{1x_1} = M_{1x_1}^{(0)} + a_1 H_{x_1},$$
$$M_{2x_1} = M_{2x_1}^{(0)} + a_2 H_{x_1}, \tag{36}$$

where

$$M_{1x_1}^{(0)} = -M_{2x_1}^{(0)}. \tag{37}$$

Substitution in the expressions for $H_{ix_1}^{\text{eff}}$ gives

$$H_{1x_1}^{\text{eff}} = H_{1x_1}^{\text{eff}(0)} + \left(-\frac{4}{Ng_x^2\mu_B^2}(z_{11}y_{11}a_1 + \tfrac{1}{2}z_{12}y'_{11}a_2) + 1\right)H_{x_1},$$
$$H_{2x_1}^{\text{eff}} = H_{2x_1}^{\text{eff}(0)} + \left(-\frac{4}{Ng_x^2\mu_B^2}(z_{11}y_{11}a_2 + \tfrac{1}{2}z_{12}y'_{11}a_1) + 1\right)H_{x_1}, \tag{38}$$

where

$$H_{1x_1}^{\text{eff}(0)} = -H_{2x_1}^{\text{eff}(0)} = -\frac{4}{Ng_x^2\mu_B^2}(z_{11}y_{11} - \tfrac{1}{2}z_{12}y'_{11})M_{1x_1}^{(0)}. \tag{39}$$

Let us denote the splitting of the doublet in the absence of external field by E_0,

$$E_0 = 2[(\tfrac{1}{2}\Delta)^2 + (\tfrac{1}{2}\mu_B g_x H_{ix_1}^{\text{eff}(0)})^2]^{1/2}. \tag{40}$$

From the expansion of the formula for M_{ix_1} in powers of H_{x_1}, one can find that

$$a_1 + a_2 = 2N\frac{(\tfrac{1}{2}\mu_B g_x)^2}{E_0}\left\{\left[1 - \tanh^2\left(\frac{E_0}{2kT}\right)\right]\frac{(\tfrac{1}{2}\mu_B g_x H_{ix_1}^{\text{eff}(0)})^2}{kTE_0} + \frac{2(\tfrac{1}{2}\Delta)^2}{E_0^2}\tanh\left(\frac{E_0}{2kT}\right)\right\} \times\left(1 + \frac{z_{11}y_{11} + \tfrac{1}{2}z_{12}y'_{11}}{E_0}\left\{\left[1 - \tanh^2\left(\frac{E_0}{2kT}\right)\right]\frac{(\tfrac{1}{2}\mu_B g_x H_{ix_1}^{\text{eff}(0)})^2}{kTE_0} + \frac{2(\tfrac{1}{2}\Delta)^2}{E_0^2}\tanh\left(\frac{E_0}{2kT}\right)\right\}\right)^{-1}. \tag{41}$$

The susceptibility χ_{x_1} along the x_1 axis of the system consisting of sublattices 1 and 2 is given by

$$\chi_{x_1} = a_1 + a_2. \tag{42}$$

Similarly, the susceptibility χ_{x_2} along the x_2 axis of the system consisting of sublattices 3 and 4 is given by

$$\chi_{x_2} = \chi_{x_1}. \tag{43}$$

Thus the susceptibilities χ_k^d of the accidental doublet along the orthorhombic crystallographic directions are

$$\chi_a^d = 2(a_1 + a_2)\cos^2\phi,$$
$$\chi_b^d = 0, \tag{44}$$
$$\chi_c^d = 2(a_1 + a_2)\sin^2\phi.$$

Note that the zero-field susceptibility in the paramagnetic state can be obtained from the formulas for χ_k^d if one takes

$$H_{ix_1}^{\mathrm{eff}(0)} = 0 \quad (i = 1, 2); \qquad E_0 = \Delta , \tag{45}$$

The transition temperature T_N can be determined from the expressions for M_{ix_1} $(i = 1, 2)$. Close to T_N the formula for M_{ix_1} $(i = 1, 2)$ can be expanded in powers of M_{ix_1} $(i = 1, 2)$ at $H_{x1} = 0$. The equations that result are linear in M_{ix_1} and to obtain a nontrivial solution for M_{ix_1}, the determinant of the coefficients has to vanish at T_N. This yields the following relation

$$\frac{2\Delta}{\frac{1}{2}z_{12}y'_{11} - z_{11}y_{11}} = \tanh\left(\frac{\Delta}{2kT_N}\right) . \tag{46}$$

Using some algebra one finds

$$T_N = \Delta\left\{k \ln\left[\left(1 + \frac{2\Delta}{\frac{1}{2}z_{12}y'_{11} - z_{11}y_{11}}\right) \Big/ \left(1 - \frac{2\Delta}{\frac{1}{2}z_{12}y'_{11} - z_{11}y_{11}}\right)\right]\right\}^{-1} , \tag{47}$$

B. Susceptibility along the $\vec{b}$ direction

The nearly accidental ground doublet has a g factor of zero along the $\vec{b}$ axis[6] and therefore does not contribute to the susceptibility in this direction. There can be, however, Van Vleck contributions to the susceptibility from each one of the elevated levels. For simplicity we shall consider only the contribution due to the lowest-lying singlet of these levels. In other words, we assume that the gap between this singlet level and those lying at higher energies is large compared with kT in the temperature range of interest. Under these conditions the formula for the susceptibility in the $\vec{b}$ direction is given by

$$\begin{aligned}\chi_b = \frac{2N\mu_B^2}{z_b}\Bigg[&\left(|\langle 0|L_y + 2S_y|1\rangle|^2 \frac{1}{E_0} + |\langle 0|L_y + 2S_y|2\rangle|^2 \frac{1}{\delta + \frac{1}{2}E_0}\right) e^{E_0/2kT} \\ &+ \left(-|\langle 1|L_y + 2S_y|0\rangle|^2 \frac{1}{E_0} + |\langle 1|L_y + 2S_y|2\rangle|^2 \frac{1}{\delta - \frac{1}{2}E_0}\right) e^{-E_0/2kT} \\ &+ \left(-|\langle 2|L_y + 2S_y|0\rangle|^2 \frac{1}{\delta + \frac{1}{2}E_0} - |\langle 2|L_y + 2S_y|1\rangle|^2 \frac{1}{\delta - \frac{1}{2}E_0}\right) e^{-\delta/kT}\Bigg] + \frac{N\mu_B^2}{z_b}|\langle 2|L_y + 2S_y|2\rangle|^2 \frac{e^{-\delta/kT}}{kT} ,\end{aligned} \tag{48}$$

where

$$z_b = e^{E_0/2kT} + e^{-E_0/2kT} + e^{-\delta/kT} . \tag{49}$$

Here $|i\rangle$ $(i = 0, 1, 2)$ mark the nearly accidental doublet and singlet levels in the order of increasing energy, δ is the separation between the center of the doublet and the singlet level, and $\langle j|L_y + 2S_y|k\rangle$ $(j, k = 0, 1, 2)$ are matrix elements connecting states $|j\rangle$ and $|k\rangle$. Note that since the g factor of the nearly accidental doublet is zero in the $\vec{b}$ direction, one has[6]

$$\langle 0|L_y + 2S_y|1\rangle = \langle 1|L_y + 2S_y|0\rangle = 0 . \tag{50}$$

δ is assumed to be temperature independent whereas the temperature dependence of E_0 is determined by Eqs. (40), (39), and (34).

C. Experimental data and determination of parameters.

The parameters involved in the theoretical formulas were deduced from the measured susceptibility curves (Fig. 1). The experimental data have been corrected for demagnetization and normalized to correspond to a zero demagnetization factor. The formulas were first fitted to the measured $\vec{a}$-$\vec{c}$ plane susceptibility through expressions (44) in the temperature range 1.4–20 K. Since both the $\vec{a}$ and $\vec{c}$ susceptibilities share the same parameters, a least-squares technique was employed to fit the two sets of data simultaneously. The temperature dependence of E_0 and $H_{ix_1}^{\mathrm{eff}(0)}$ involved in the susceptibility through Eq. (41) was calculated from formulas (39) and (40) after deriving $M_{ix_1}^{(0)}$ by applying an iteration method on Eq. (34). The following results were obtained:

$$\begin{aligned} &g_x = 7.7 \pm 0.4 , \\ &\phi = 17^\circ \pm 3^\circ , \\ &\Delta = (7.9 \pm 7.9) \times 10^{-16}\ (\mathrm{erg}) = 5.7 \pm 5.7\ (\mathrm{K}) , \\ &z_{11}y_{11} = (-27.2 \pm 6.0) \times 10^{-16}\ (\mathrm{erg/spin}) = -19.7 \pm 4.3\ (\mathrm{K/spin}) , \\ &\tfrac{1}{2}z_{12}y'_{11} = (12.4 \pm 3.0) \times 10^{-16}\ (\mathrm{erg/spin}) = 8.9 \pm 2.2\ (\mathrm{K/spin}) . \end{aligned} \tag{51}$$

The quoted errors are statistical and indicate two standard deviations. Though the least-squares

fit was done in the temperature range 1.4–20 K the theoretical $\vec{a}$ and $\vec{c}$ susceptibility curves calculated using parameters (51) seem to be in good agreement with the experimental data in the whole range 1.4–80 K (Fig. 1).

In fitting formula (48) to the experimental susceptibility in the $\vec{b}$ direction we employed the temperature dependence of E_0 calculated using parameters (51). The least-squares fit of χ_b was done in the whole range 1.4–80 K and the agreement between the calculated and experimental curves is excellent (see Fig. 1). From this fit the following additional parameters were obtained:

$$\begin{aligned}
&\delta = (64.9 \pm 4.0) \times 10^{-16}\ (\text{erg}) = 47.0 \pm 2.9\ (\text{K}),\\
&|\langle 0|L_y + 2S_y|2\rangle|^2 = |\langle 2|L_y + 2S_y|0\rangle|^2\\
&\qquad = 5.35 \pm 0.30,\\
&|\langle 1|L_y + 2S_y|2\rangle|^2 = |\langle 2|L_y + 2S_y|1\rangle|^2\\
&\qquad = 4.77 \pm 0.40,\\
&|\langle 2|L_y + 2S_y|2\rangle|^2 = 6.52 \pm 3.20.
\end{aligned} \tag{52}$$

The errors quoted here are statistical and indicate two standard deviations. From parameters (51) it is evident that the ferromagnetic intrasublattice coupling between Fe^{2+} spins is stronger than the intersublattice antiferromagnetic interaction. By using Eqs. (34) and (39) we calculate the Fe^{2+}-Fe^{2+} effective fields at $T=0$ K in the spontaneously ordered configuration

$$\begin{aligned}
&H^{f}_{ix_1} = H^{f}_{jx_2} = \left| \frac{4}{N g_x^2 \mu_B^2} z_{11} y_{11} M^{(0)}_{1x_1}(T=0\ \text{K}) \right|\\
&\qquad = 17.5 \pm 5.2\ \text{kOe}\\
&i = 1,2 \quad j = 3,4\\
&H^{af}_{ikx_1} = H^{af}_{jlx_2} = \left| \frac{4}{N g_x^2 \mu_B^2} \tfrac{1}{2} z_{12} y'_{11} M^{(0)}_{1x_1}(T=0\ \text{K}) \right|\\
&\qquad = 8.0 \pm 2.7\ \text{kOe}\\
&i,k = 1,2, \quad j,l = 3,4\\
&i \neq k, \quad j \neq l.
\end{aligned} \tag{53}$$

Here, $H^{f}_{ix_1}$, $H^{f}_{jx_2}$ and $H^{af}_{ikx_1}, H^{af}_{jlx_2}$ are the magnitudes of the ferromagnetic and antiferromagnetic fields, respectively, and the indices i, j, k, l indicate the sublattices. The magnitude of the total Fe^{2+}-Fe^{2+} effective field H^{eff}_{Fe} at $T=0$ K is (note that $H^{eff}_{Fe} = H^{eff(0)}_{1x_1}$)

$$H^{eff}_{Fe} = H^{f}_{11x_1} + H^{af}_{12x_1} = 25.5 \pm 7.9\ \text{kOe}. \tag{54}$$

Similarly, the magnitude of the Fe^{2+}-Fe^{2+} effective field in the field-induced paramagnetic state at $T=0$ K can be calculated. Since the nearly accidental ground doublet of the Fe^{2+} ions has a zero g factor in the $\vec{b}$ direction, only external fields in the $\vec{a}$-$\vec{c}$ plane can practically induce paramagnetic configurations at moderate fields. With the Fe^{2+} moments being confined to the local principal axes x_1 and x_2 of the g tensor at the two magnetically nonequivalent sites, respectively, they cannot be aligned in the direction of an external field. When high magnetic field is applied along the $\vec{a}$ or $\vec{c}$ axes, two out of the four sublattices will be reversed along their spin easy directions resulting in the paramagnetic F_xC_z or F_zC_x configurations, respectively.[5] If the external field is high enough to induce a splitting of the nearly accidental ground doublet that is much larger than its crystal-field splitting Δ then the sublattice magnetizations $M_{ix_1}(T=0\ \text{K})$ $i=1,2$ and $M_{jx_2}(T=0\ \text{K})$ $j=3,4$ will approach their full value of $\frac{1}{4} N g_x \mu_B S$ and the magnitude of the total Fe^{2+}-Fe^{2+} effective field $H^{eff}_{ac\,Fe}$ will be given by

$$H^{eff}_{ac\,Fe} = \left| \frac{\frac{1}{2}(z_{11} y_{11} + \frac{1}{2} z_{12} y'_{11})}{g_x \mu_B} \right| = 10.4 \pm 5.2\ \text{kOe}. \tag{55}$$

In formulas (53)–(55), both exchange and dipolar contributions are included. In order to assess the importance of the dipolar contribution we calculated the dipolar field component $H^{eff}_{a\,Fe\,dip}$ and $H^{eff}_{c\,Fe\,dip}$ along the local-spin easy axis in the two field-induced paramagnetic configurations F_xC_z and F_zC_x, respectively. By taking a magnetic moment of $3.85\mu_B$ per Fe^{2+} ion one has

$$\begin{aligned}
&H^{eff}_{a\,Fe\,dip} = -2.9\ \text{kOe},\\
&H^{eff}_{c\,Fe\,dip} = -5.7\ \text{kOe},
\end{aligned} \tag{56}$$

where the (–) signs indicate that the dipolar fields are in opposite direction to the induced Fe^{2+} magnetic moments. It can be seen that the dipolar contribution is small and that the exchange interactions constitute the dominant part of the Fe^{2+}-Fe^{2+} bilinear coupling.

The major part of the spontaneous splitting E_0

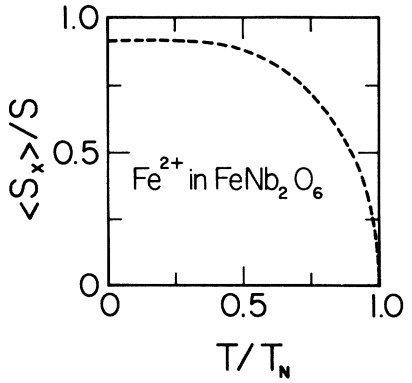

FIG. 5. Calculated temperature dependence of $\langle S_x \rangle / S$ for Fe^{2+} in $FeNb_2O_6$ using the parameters derived in the text.

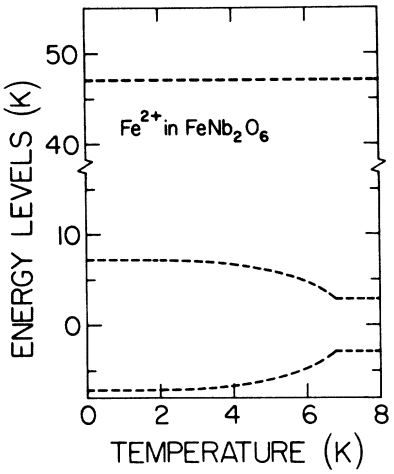

FIG. 6. Calculated temperature dependence of the lowest-lying Fe^{2+} energy levels in $FeNb_2O_6$ using the parameters derived in the text.

of the nearly accidental ground doublet at low temperature is due to the Fe^{2+}-Fe^{2+} bilinear coupling. It is the competition between this temperature-dependent splitting and the constant crystal field splitting Δ that determines the main features of the temperature dependence of the sublattice magnetization. The temperature dependence of the spontaneous sublattice magnetization calculated by using formulas (34) and (39) with parameters (51) is shown in Fig. 5. It is obvious from formula (34) that the smaller the ratio $\Delta/\mu_B g_x H_{ix_1}^{\text{eff}}$ the closer will the sublattice magnetization M_{ix_1} come to its full value of $\frac{1}{4} N g_x \mu_B S$ at $T=0$ K. The calculated temperature dependence of the splitting of the nearly accidental ground doublet can be seen from Fig. 6. The spontaneous temperature dependence of the energy levels in Fig. 6 was calculated by using formulas (29) and (39), with parameters (51) and (52), after deriving $M_{ix_1}^{(0)}$ by applying an iteration method on Eq. (34).

The calculation of T_N using formula (47) with parameters (51) yields $T_N = 6.8$ K which is higher than the ordering temperature associated with the maximum in $d\chi/dT$. This is probably due in part to the approximation employed in the mean-field theory which provides a reasonable description only of the main features of the magnetic behavior of a spin system.

V. DISCUSSION

We have shown that the main features of the magnetic behavior of $FeNb_2O_6$ at low temperatures can be accounted for in the mean-field approximation assuming a four-sublattice antiferromagnetic spin configuration and a nearly accidental ground doublet for the Fe^{2+} ions in this material. The four sublattice model is in disagreement with the collinear antiferromagnetic spin structure along the $\vec{a}$ axis deduced by Weitzel from his neutron diffraction measurements on powders.[3] Note, however, that a doubling of the unit cell that he found to take place along the $\vec{b}$ axis is not a doubling of a spin configuration that originates in the crystallographic space group *Pbcn*,[5] but rather one of a lower symmetry. Reminiscent of the crystallographically isostructural $MnNb_2O_6$,[3,11] it seems that because of the insufficient resolution in the powder-diffraction patterns possible deviations from a collinear spin structure are hard to detect. Neutron-diffraction experiments on single crystals are clearly needed to determine the detailed spin configuration of $FeNb_2O_6$.

The low-temperature magnetic behavior of $FeNb_2O_6$ is highly influenced by the Fe^{2+} ions occupying the lowest crystal-field levels. In our model, their magnetic moments at low temperatures are confined to the local direction of the nonzero component of the g tensor at each site. It remains to be seen whether this model in its present form can account for the experimental magnetic-phase diagram or whether it needs to be modified to provide a better approximation of the Fe^{2+} spins in $FeNb_2O_6$.

Our least-squares fit of the theoretical formulas to the experimental susceptibility was not so sensitive to the magnitude of the crystal-field splitting Δ of the ground doublet which resulted in a relatively high statistical error bar on that parameter [see (51)]. A nonzero crystal-field splitting Δ of the ground-doublet results in a nonzero susceptibility in the $\vec{a}$-$\vec{c}$ plane at $T=0$ K (Fig. 1) and in an unsaturated spontaneous sublattice magnetization at $T=0$ K (Fig. 5). Experimentally, this should manifest itself in a relatively high magnetic field needed to approach saturation on magnetization versus field curves and in a field dependence of the intensity of neutron diffraction lines even at very low temperatures. In view of its importance it would be useful to obtain a better determination of Δ by trying other techniques that might be more sensitive to this parameter such as magneto-optical studies or specific-heat measurements. Some information on the crystal-field levels of Fe^{2+} in $FeNb_2O_6$ was obtained by Eibschütz, Ganiel, and Shtrikman in earlier studies of the temperature dependence of the quadrupole splitting of the Mössbauer line in a powder sample.[12] Their calculated energy level scheme for the Fe^{2+} ions in $FeNb_2O_6$ clearly shows that the three lowest-lying crystal-field levels (a lower singlet and an upper doublet 19 K apart) are relatively isolated from the higher levels and therefore can be regarded as essentially the only populated levels at a suf-

ficiently low temperature. As we have shown, the magnetic properties at low temperatures are indeed dominated by the Fe^{2+} ions occupying the three lowest-lying crystal-field levels. The quadrupole splitting of the Mössbauer line, however, obtained at temperatures higher than 25 K, is probably not sensitive enough to the crystal-field splittings between the three lowest-lying singlets, and therefore, the resulting calculated energy-level scheme can be regarded only as a first approximation.

As indicated already, the Fe^{2+} ions are arranged in Fe-O layers that are parallel to the crystallographic $\vec{b}$-$\vec{c}$ plane and are separated from neighboring layers along the $\vec{a}$ axis. In the analysis we considered only interactions between Fe^{2+} ions within the layers and neglected interlayer coupling which is expected to be weaker. The Fe^{2+}-Fe^{2+} bilinear interactions in $FeNb_2O_6$ are essentially of an exchange type with a small dipolar contribution. We found the Fe^{2+}-Fe^{2+} intrasublattice ferromagnetic coupling to be stronger than the antiferromagnetic intersublattice interaction as in the isostructural $NiNb_2O_6$.[5]

The parameters (51) we obtained from the least-squares fit of the theoretical expressions to the experimental data yield a Néel temperature $T_N = 6.8$ K which is higher than the one found experimentally. This is probably due in part to the approximations inherent in the mean-field theory which is known to provide a reasonable description only of the main features of the magnetic behavior of a spin system.

The magnetic properties of single crystals of $FeNb_2O_6$ have been studied and presented in this paper for the first time. Additional and complementary information can be obtained by employing other experimental techniques. In particular, measurements on $FeNb_2O_6$ single crystals are needed to verify the implications of the four sublattice antiferromagnetic structure and the nearly accidental ground-doublet model proposed in our analysis. Some of these experiments are now in progress.

ACKNOWLEDGMENTS

Many thanks are due to Dr. D. Mukamel for useful suggestions and helpful discussions during the course of this work. The authors would like to express their gratitude also to Professor R. Hornreich and Professor S. Shtrikman for correspondence and comments on the manuscript.

---

*Present address: Dept. of Physics and Astronomy, University of Georgia, Athens, Ga. 30602.

[1]K. Brandt, Ark. Kemi Mineral. Geol. 17A, No. 15, 1 (1943).
[2]H. Schröcke, N. Jahrb, Mineral. Abh. 106, 1 (1966).
[3]V. H. Weitzel, Z. Anorg. Allg. Chem. 380, 119 (1971).
[4]B. M. Wanklyn, B. J. Garrard, and G. Garton, Mater. Res. Bull. 11, 1497 (1976).
[5]I. Yaeger, A. H. Morrish, and B. M. Wanklyn, Phys. Rev. B 15, 1465 (1977).
[6]J. S. Griffith, Phys. Rev. 132, 316 (1963).
[7]R. M. Hornreich, B. M. Wanklyn, and I. Yaeger, Int. J. Magn. 2, 77 (1972).
[8]I. Yaeger, J. E. Rives, D. P. Landau, B. M. Wanklyn, and B. J. Garrard (unpublished).
[9]K. Olbrychski, Phys. Status Solidi 3, 1868 (1963).
[10]See, for instance, E. F. Bertaut, Acta Crystallogr. A 24, 217 (1968).
[11]O. V. Nielsen, B. Lebech, F. Krebs Larsen, L. M. Holmes, and A. A. Ballman, J. Phys. C 9, 2401 (1976).
[12]M. Eibschütz, U. Ganiel, and S. Shtrikman, Phys. Rev. 156, 259 (1967).